Conference on Biomaterials
・Effects of Fluorine Doping of Amorphous Diamond-Like Carbon Films on Platelet Adhesion and Activation
S. Yohena, T. Hasebe, T. Saito, Y. Matsuoka, A. Kamijo,__K. Takahashi, T. Suzuki
CMCTF2005: International Conference on Metallurgical Coatings and Thin Films (USA)

＜国内学会＞
・フッ素添加 Diamond-like Carbon 膜表面における血小板付着および活性化抑制効果
齊藤俊哉，長谷部光泉，松岡義明，饒平名智士，上條亜紀，高橋孝喜，鈴木哲也
第 18 回 ダイヤモンドシンポジウム
・フッ素添加 DLC 膜上におけるタンパク質の吸着と血小板の付着及び活性化の評価（最優秀賞受賞）
饒平名智士，長谷部光泉，齊藤俊哉，松岡義明，上條亜紀，高橋孝喜，鈴木哲也
第 18 回 ダイヤモンドシンポジウム
・Diamond-like carbon (DLC) コーティングを用いた医療材料の生体適合性・抗血栓性評価方法確立の重要性
鈴木哲也、長谷部光泉、齊藤俊哉、饒平名 智士、松岡義明、上條亜紀、高橋孝喜
日本学術振興会化学研究費基板研究 C アモルファス炭素系薄膜の化学：第 2 回企画調査研究会
・フッ素添加 DLC の抗血栓性メカニズム解明の試み
長谷部光泉、饒平名 智士、齊藤俊哉、松岡義明、上條亜紀、高橋孝喜、鈴木哲也
日本学術振興会化学研究費基板研究 C アモルファス炭素系薄膜の化学：第 2 回企画調査研究会

G：知的財産権の出願・登録情報
なし

厚生労働科学研究費補助金（医薬品・医療機器等レギュラトリーサイエンス総合研究事業）

分担研究報告書

臍帯血の供給に関する研究

分担研究者
十字　猛夫　日本赤十字社中央血液研究所　所長
高梨美乃子　東京都赤十字血液センター　技術部長

研究要旨：
臍帯血バンク運営上、提供され調製保存施設に受け入れられる臍帯血のうち 50-60%のみが移植用として調製保存される。臍帯血の有効活用のために、移植のための細胞数基準に至らない場合には研究用に活用すべく研究者とのネットワークを構築する。全体の約 20%を研究用に譲渡することができた。

A：研究目的

臍帯血バンク事業では採取協力施設の妊婦さんらに広く協力を呼びかける一方、実際に移植用としての細胞数基準に達しない臍帯血は凍結保存に至らない。この様な臍帯血をできる限り早く研究者に提供するシステムを構築する。

B：研究方法

臍帯血バンクへの臍帯血提供の同意には、移植に至らない場合の研究用使用も含まれている。ただし移植医療に貢献できる研究でなければならない。東京都赤十字血液センター臍帯血バンクでは、研究用譲渡を希望する研究者から提出された研究計画書、当該施設の倫理委員会での研究承認書類等を臍帯血バンク研究審査部会に回覧し、2/3 以上の賛成多数をもって承認とした。あらかじめ承認した研究者に対して、臍帯血が研究用と判断した時点で連絡した。

C：研究結果

臍帯血は容量が十分採取された場合に臍帯血バンクへ搬送される。さらに細胞数が十分あれば移植目的に保存可能と判断して、調製を開始する。保存されたのは受入数 641 件の 60.7%、389 件であった。252 件の保存にいたらない理由は細胞数不足、クロット、受入までに 24 時間以上経過、母既往歴、家族歴、調製不良、感染症スクリーニング陽性である。クロット形成を認める検体は有核細胞回収率が低い可能性があり、その他の事由は調製開始時には未確定のこともあり、研究用に提供するのには細胞数不足の臍帯血が適当であると考えられた。細胞数基準で調製できないものは 252 中 172 件（68.3%）、全体の 26.8%であった。また、この判定は臍帯血採取後 24 時間以内に行われるため、研究者への譲渡時点では臍帯血採取後おおよそ 24 時間内外であった。

2004 年 4 月-2005 年 1 月までの実績を以下に示す。

	臍帯血受入数	調製保存数	受入数-保存数	研究用譲渡数	譲渡先数
4 月	58	33	25	19	6
5 月	50	28	22	13	4
6 月	68	36	32	21	5
7 月	59	33	26	14	5
8 月	80	54	26	13	3
9 月	81	54	27	10	5
10 月	70	43	27	11	4
11 月	60	40	20	9	4
12 月	62	39	23	10	5
1 月	53	29	24	6	4
計	641	389	252	126	------

細胞数不足で調製できない臍帯血 172 件のうち 126 件を研究用に提供することができ、その利用率は 73.3%であった。譲渡先数は、各研究者により学会や研究環境に影響され変動した。

D：考察

臍帯血が研究用に譲渡できるかは予測が困難である。研究者によっては研究曜日が限られており、指定曜日および前回譲渡からの時間経過を勘案して臍帯血バンクから研究者宛に連絡した。残念ながらそれぞれの研究計画と一致しない可能性もあると考えられた。

妊産婦の意志を尊重するためにも、臍帯血の細胞数が基準に満たない場合には有効活用を図るべきである。臍帯血バンクでも各種調製保存手技のバリデーションのために一部が使用されるが、更に研究にも協力し、よって移植医療に貢献すべきと考える。臍帯血が移植目的に保存されない理由のうちクロットについては、今後の検討事項である。

E：結論

臍帯血バンクの全臍帯血受入件数の内26.8％は細胞数基準に満たないために研究用譲渡の対象となった。実際に研究者に譲渡したのは全体の19.7％であった。

F：研究発表

なし

G：知的所有権の出願・取得情報

なし

Ⅲ．　研究成果の刊行に関する一覧

研究成果の刊行に関する一覧表(論文)

発表者氏名	論文タイトル名	発表誌名	巻名	ページ	出版年
Saito T, Hasebe T, Yohena S, Matsuoka , Kamijo A, Takahashi K, Suzuki T.	Antithrombogenicity of fluorinated diamond-like carbon films.	Diamond & Related Materials			in press
Hosoya N, Qiao Y, Hangaishi A, Wang , Nannya Y, Sanada M, Kurokawa M, Chiba S, Hirai H, Ogawa S.	Identification of a SRC-like tyrosine kinase gene, FRK, fused with ETV6 in a patient with acute myelogenous leukemia carrying a t(6;12)(q21;p13) translocation.	Genes Chromosomes Cancer	42	269-279	2005
Hori A, Kanda Y, Goyama S, Onishi Y, Komeno Y, Mitani K, Kishi Y, Ogawa S, mataki O, Chiba S, Kojima R, Hamaki T, Sakiyama M, Kami M, Makimoto A, Tanosaki R, Takaue Y, Hirai H.	A prospective trial to evaluate the safety and efficacy of pravastatin for the treatment of refractory chronic graft-versus-host disease.	Transplantation	79	372-374	2005
Yanada M, Emi N, Naoe T, Sakamaki H, seki T, Hirabayashi N, Karasuno T, Chiba S, Atsuta Y, Hamajima N, Takahashi S, Kato S.	Allogeneic myeloablative transplantation for patients aged 50 years and over.	Bone Marrow Transplantation	34	29-35	2004
Morishima Y, Ogura M, Nishimura M, Yazaki F, Bessho M, Mizoguchi H, Chiba S, Hirai H, Tauchi T, Urabe A, Takahashi M, Ohnishi K, Yokozawa T, Emi N, Hirano M, Shimazaki C, Nakao S, Kawai Y, Fujimoto M, Taguchi H, Jinnai I, Ohno R.	Efficacy and safety of imatinib mesylate for patients in the first chronic phase of chronic myeloid leukemia: results of a Japanese phase II clinical study.	Int J Hematol.	80	261-266	2004
Endo-Matsubara M, Ogawa S, Sasaki K, Takahashi T, Chiba S, Hirai H.	Immature granulocyte fraction in the peripheral blood is a practical indicator for mobilization of CD34(+) cells.	Am J Hematol	7	223-228	2004
Yamaguchi Y, Kurokawa M, Imai Y, Izutsu K, Asai T, Ichikawa M, Yamamoto G, Nitta E, Yamagata T, Sasaki K, Mitani K, Ogawa S, Chiba S, Hirai H.	AML1 Is Functionally Regulated through p300-mediated Acetylation on Specific Lysine Residues.	J Biol Chem.	279	15630-15638	2004
Sakata-Yanagimoto M, Kanda Y, Nakagawa M, Asano Y, Nakagawa M, Sakata-Yanagimoto M, Kandabashi K, Izutsu K, Imai Y, Hangaishi A, Kurokawa M, Tsujino S, Ogawa S, Aoki K, Chiba S, Motokura T, Hirai H.	Predictors for severe cardiac complications after hematopoietic stem cell transplantation.	Bone Marrow Transplant	33	1043-1047	2004

研究成果の刊行に関する一覧表 (論文)

発表者氏名	論文タイトル名	発表誌名	巻名	ページ	出版年
Ogawa N, Kanda Y, Matsubara M, Asano Y, Nakagawa M, Sakata-Yanagimoto M, Kandabashi K, Izutsu K, Imai Y, Hangaishi A, Kurokawa M, Tsujino S, Ogawa S, Aoki K, Chiba S, Motokura T, Hirai H.	Increased incidence of acute graft-versus-host disease with the continuous infusion of cyclosporine A compared to twice-daily infusion.	Bone Marrow Transplant	33	549-552	2004
Kunisato A, Chiba S, Saito T, Kumano K, Nakagami-Yamaguchi E, Yamaguchi T, Hirai H.	Stem cell leukemia protein directs hematopoietic stem cell fate.	Blood	103	3336-3341	2004
Kojima R, Kami M, Nannya Y, Kusumi E, Sakai M, Tanaka Y, Kanda Y, Mori S, Chiba S, Miyakoshi S, Tajima K, Hirai H, Taniguchi S, Sakamaki H, Takaue Y.	Incidence of invasive aspergillosis after allogeneic hematopoietic stem cell transplantation with a reduced-intensity regimen compared with transplantation with a conventional regimen.	Biol Blood Marrow Transplant	10	645-652	2004
Kawazu M, Kanda Y, Nannya Y, Aoki K, Kurokawa M, Chiba S, Motokura T, Hirai H, Ogawa S.	Prospective comparison of the diagnostic potential of real-time PCR, double-sandwich enzyme-linked immunosorbent assay for galactomannan, and a (1→3)-β-D-glucan test in weekly screening for invasive aspergillosis in patients with hematological disorders.	J Clin Microbiol	42	2733-2741	2004
Ichikawa M, Asai T, Saito T, Yamamoto G, Seo S, Yamazaki I, Yamagata T, Mitani K, Chiba S, Ogawa S, Kurokawa M, Hirai H.	AML-1 is required for megakaryocytic maturation and lymphocytic differentiation, but not for maintenance of hematopoietic stem cells in adult hematopoiesis.	Nature Med.	10	299-304	2004
Haraguchi K, Takahashi T, Hiruma K, Kanda Y, Tanaka Y, Ogawa S, Chiba S, Miura O, Sakamaki H, Hirai H.	Recovery of Valpha24(+) NKT cells after hematopoietic stem cell transplantation.	Bone Marrow Transplant	34	595-602	2004
Goyama S, Yamaguchi Y, Imai Y, Kawazu M, Nakagawa M, Asai T, Kumano K, Mitani K, Ogawa S, Chiba S, Kurokawa M, Hirai H.	The transcriptionally active form of AML1 is required for hematopoietic rescue of the AML1-deficient embryonic para-aortic splanchnopleural (P-Sp) region.	Blood	104	3558-3564	2004

Ⅳ. 研究成果の刊行物・別刷

Available online at www.sciencedirect.com

SCIENCE DIRECT®

Diamond & Related Materials xx (2004) xxx–xxx

DIAMOND AND RELATED MATERIALS

www.elsevier.com/locate/diamond

Antithrombogenicity of fluorinated diamond-like carbon films

T. Saito[a,1], T. Hasebe[a,b,*,1], S. Yohena[a], Y. Matsuoka[a], A. Kamijo[c], K. Takahashi[c], T. Suzuki[a]

[a]*Center for Materials Science, Department of Mechanical Engineering, Keio University School of Science and Technology, 3-14-1 Hiyoshi, Kohoku-ku, Yokohama, Kanagawa 223-8522, Japan*

[b]*Department of Radiology, Tachikawa Hospital, 4-2-22 Nishiki-cho, Tachikawa, Tokyo 190-8531, Japan*

[c]*Department of Transfusion Medicine, the University of Tokyo Hospital, 7-3-1 Hongo, Bunkyo-ku, Tokyo 113-8655, Japan*

Abstract

Effects of doping with fluorine to diamond-like carbon (DLC) films on the antithrombogenicity were investigated by changing its content. Fluorinated DLC (F-DLC) films were prepared on silicon (Si) substrates using radio frequency (RF) plasma enhanced chemical vapour deposition (CVD) by changing the ratio of hexafluoroethane (C_2F_6) and acetylene (C_2H_2). The contact angle measurements of human whole blood droplet on Si, DLC and F-DLC were 24.2°, 60.8° and 95.3°, respectively. Furthermore, the static evaluation of F-DLC films incubated with platelet-rich plasma (PRP) showed dramatic reduction of platelet adhesion and activation on the surface. It was found that the addition of fluorine into DLC films much improved antithrombogenicity, which was clearly shown by scanning electron microscopy (SEM) with statistical analysis. F-DLC coating can be a great candidate for developing antithrombogenic surfaces in blood contacting materials.

Keywords: Fluorinated diamond-like carbon; Hydrophobicity; Platelet adhesion; Antithrombogenicity

1. Introduction

Biomaterial implants such as vascular grafts, artificial heart valves or interventional devices (stents, guidewires and catheters) have been gaining widespread use with development of medical engineering. Thrombogenic complication remains as one of the main problems for blood contacting implants, which triggers the life-threatening device failure. For example, it has been reported that the restenosis after coronary stenting statistically occurs 20% to 40% [1–4]. Recent study has shown that the thrombus formation after intraarterial stent implantation provides a stimulus for neointimal hyperplasia and, if excessive, can result in stent thrombosis at sites of coronary stenting in humans [4]. Surface modification techniques are indispensable for improving both the mechanical and physical properties of these implants in direct contact with the blood and tissue.

Recently, diamond-like carbon (DLC) films have received much attention because of their antithrombogenicity, which inhibits platelet adhesion and activation [5–7]. However, the blood coagulation mechanism on DLC films in biological environment has not been well understood so far. There have been several reports that cell adhesion on DLC films is related to surface energy and wettability [8–12]. They suggested that hydrophobic surface tends to inhibit blood cell adsorption. As for hydrophobic property, it is well known that fluorocarbon polymers present great water-shedding characteristics. Thus, we consider that the addition of fluorinate has potential to develop haemocompatibility of materials.

2. Experimental

2.1. Film preparations and characterization

Conventional DLC and fluorinated DLC (F-DLC) films were prepared on Silicon (Si) substrates using radio

* Corresponding author. Center for Materials Science (Suzuki lab.), Department of Mechanical Engineering, Keio University School of Science and Technology, 3-14-1 Hiyoshi, Kohoku-ku, Yokohama, Kanagawa 223-8522, Japan. Tel.: +81 45 563 1141; fax: +81 45 566 1495.

E-mail address: teru_hasebe@hotmail.com (T. Hasebe).

[1] Both authors contributed equally to this work.

0925-9635/$ - see front matter © 2004 Elsevier B.V. All rights reserved.
doi:10.1016/j.diamond.2004.09.017

frequency (RF) plasma enhanced chemical vapour deposition (CVD) method by changing the ratio of hexafluoroethane (C_2F_6) and acetylene (C_2H_2). The RF (13.56 MHz) power and total pressure were fixed at 200 W and 13.3 Pa, respectively. DLC films were deposited from C_2H_2 and F-DLC films from a mixture of C_2H_2 and C_2F_6, and the thickness of DLC and F-DLC films was 40 to 50 nm, respectively. According to partial pressure of C_2F_6, each F-DLC film was denoted as follows: for example, F-DLC20 indicates that F-DLC films were deposited under partial pressure of C_2F_6 at 20% of the total pressure.

Surface chemical compositions and bonding states of DLC and F-DLC films were measured by the X-ray photoelectron spectroscopy (XPS; JPS-9000MX, JEOL). The wettability of Si, DLC and F-DLC80 were evaluated by measuring the static contact angles between a droplet of human whole blood (10 μl) and the samples surfaces.

2.2. Platelet adhesion and activation

Human whole blood (45 ml) from a healthy volunteer without any medication for at least 10 days was collected and mixed with 5 ml of acid-citrate-dextrose (ACD), and then the blood was centrifuged at 180 ×*g* for 10 min to separate the blood corpuscles, and the resulting platelet-rich plasma (PRP) was prepared. Subsequently, the rest of whole blood was centrifuged at 2000 ×*g* for 20 min to obtain the platelet-poor plasma (PPP). The density of platelets in PRP was adjusted to a concentration of 2×10^5 cells/μl by diluting with PPP. After rinsing samples with phosphate-buffered saline (PBS), the samples disks with a surface area of 100 mm^2 were incubated in a 24-wells plate with 2 ml of adjusted PRP for 60 min with 5% of CO_2 gas at 37 °C (n=5 disks for each sample). Thereafter, the supernatant was discarded, and the samples were washed with PBS. The adherent platelets were then fixed with 1 ml of freshly prepared 1.0% of glutardialdehyde for 60 min at room temperature. After fixation, the samples were washed and dehydrated in a graded ethanol series (20%, 40%, 60%, 80%, 100% and 100% for 15 min each), as described previously [13]. Dehydrated materials were put in a vacuum chamber and dried overnight. The entirely dried materials were coated with gold and investigated by a scanning electron microscopy (SEM; S-3100H, HITACHI).

Adhering platelets were manually counted on photographs per unit area (6000 μm^2). Results of the experiments are expressed as means of counts/unit area and standard error (SE). Values were compared statistically by unpaired t test. Results with $P<0.05$ were considered to be statistically significant. Additionally, the morphological shape changes were categorized to Goodman et al. and

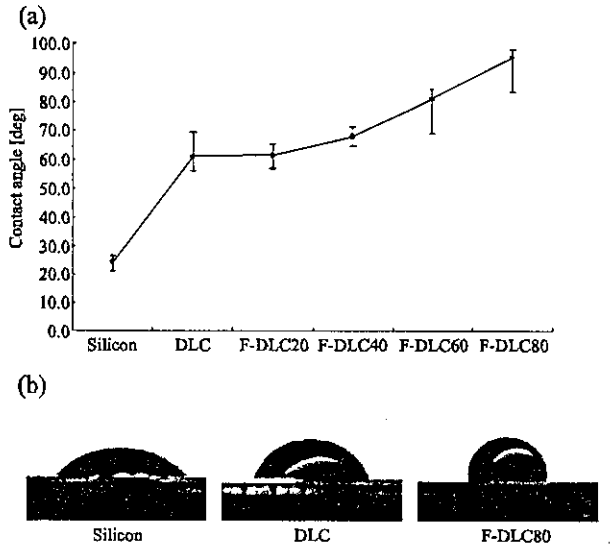

Fig. 2. Contact angle measurements of 10-μl whole human blood droplet on the sample surface (wettability). The values of contact angle dramatically increased with increasing the ratio of doped fluorine (a). F-DLC80 showed the most hydrophobic property (b).

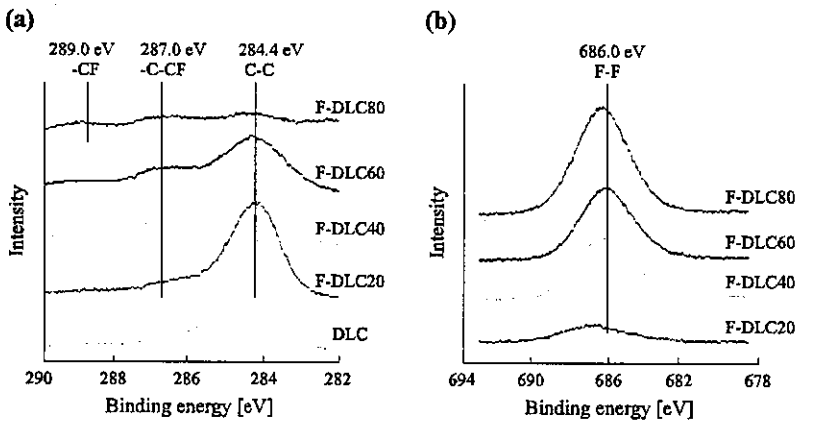

Fig. 1. XPS spectra of DLC, F-DLC20, F-DLC40, F-DLC60 and F-DLC80. (a) C1s XPS. (b) F1s XPS.

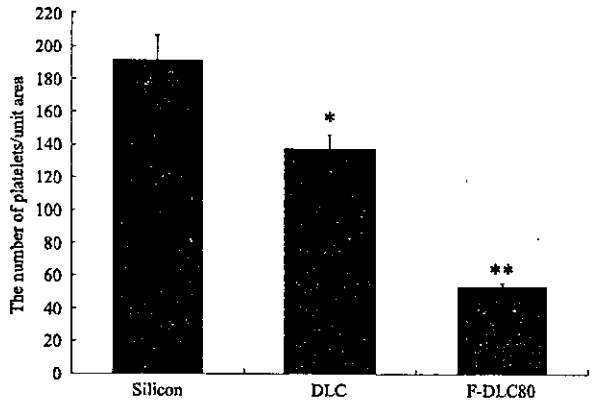

Fig. 3. The number of adhering platelets counted on Si substrate, DLC and F-DLC80. The number of platelets per unit area (6000 μm^2) was counted. The values are the mean of five areas of each sample, while the error bars denote the standard deviation. * denotes significant difference from control Si substrate (*P<0.05) .** denotes significant difference from Si or DLC (**P<0.001).

Allen et al. [14,15] as (I) round or discoid, (II) dendritic or early pseudopodial, (III) spread-dendritic or intermediate pseudopodial, (IV) spreading or late pseudopodial and (V) fully spread.

3. Results and discussion

3.1. Chemical compositions and bonding

Fig. 1(a) and (b) shows the local spectra of C1s and F1s for DLC, F-DLC20, F-DLC40, F-DLC60 and F-DLC80 by XPS. The horizontal axis corresponds to binding energy [eV] and the vertical axis to intensity. By taking curve fitting to each spectrum, they were well decomposed into main three peaks, which centered at ~284.4, ~287.0 and ~289.0 eV, respectively. Due to the surface contamination and charging effect during XPS analysis, it is very complex and also still controversial to identify these peaks.

As shown in Fig. 1, the peak intensity for C–C bond (284.4eV) gradually decreased (Fig. 1(a)) and the peak intensity for F–F bond (686.0 eV) gradually increased (Fig. 1(b)) with increasing pressure of C_2F_6 gas during deposition. This indicates that the pressure of C_2F_6 influences the ratio of fluorine on the topmost surface of films. Furthermore, in the spectra of F-DLC films, there were some peaks indicating bonds of carbon and fluorine. The spectra of F-DLC20, F-DLC40 and F-DLC60 showed the existence of C–CF bond (287.0 eV) as well as C–C bond. The spectrum of F-DLC80 showed the existence of C–F bond (289.0 eV) in addition to C–CF and C–C bonds. Bonding structures of carbon and fluorine show low polarizability, which leads to low surface energy with increasing the hydrophobicity of F-DLC films.

3.2. Contact angle measurements

Fig. 2 shows the results of contact angle measurements for three different samples. These results indicated the dramatic improvement of wettability for DLC and F-DLC films. The contact angles of human blood on Si, DLC and F-DLC80 were 24.2°, 60.8° and 95.3°, respectively. For the DLC films, the contact angle increased by 2.51 times compared to that of Si substrate. In particular, F-DLC80 is the most hydrophobic, and the contact angle for F-DLC80 increased by 3.94 times compared to that of Si.

The more hydrophobic a surface is, the higher the interfacial free energy between the solid and liquid phases. The interfacial free energy determines the wetting characteristics and hence the wall shear stress generated when the liquid comes into contact with the surface. It is considered that the polarization of C–F and C–CF bonds on the topmost surface of F-DLC80, proven by the XPS analysis, can lower the surface energy and the results in the increase in contact angles.

3.3. Platelet adhesion and activation

Platelets play a pivotal role in thrombogenicity of biomaterials in blood contacting applications, and the reduction of platelet adhesion and activation is determinant for the eventual success of any application. The initial local response to foreign surface in the body is mainly catalyzed by surface-absorbed proteins, which trigger numerous processes such as cellular activation, inflammatory and complement activation and attraction of circulating platelets.

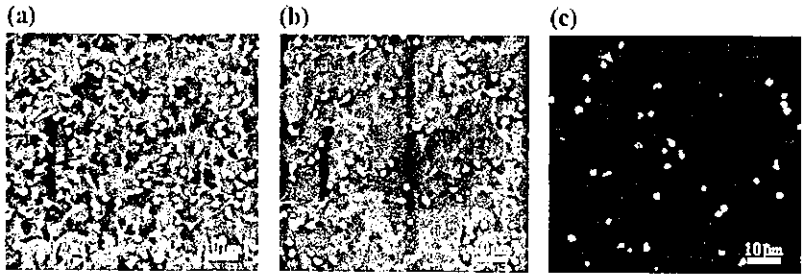

Fig. 4. Morphology of adherent platelets on (a) Si, (b) DLC and (c) F-DLC sufaces (60 min incubation in PRP) observed using SEM. Si substrate: dense platelet layers (categories IV and V). DLC: lower density of platelets compared to Si (categories III to V). F-DLC80: a few platelets (categories uniformly I to V).

During activation, the platelets attach to the sample surface, and they change in shape in developing pseudopodia versus their activation level [12]. Thus, the investigation of platelet adhesion must support the thrombogenicity evaluation of biomaterials.

Fig. 3 shows the adherent platelets counts on the three different samples by SEM. This result clearly demonstrated that the number of platelets per unit area for DLC or F-DLC80 was significantly smaller compared to that of Si substrate ($P<0.05$ and $P<0.001$, respectively). In addition, the number of platelets on F-DLC80 was significantly smaller than that of DLC ($P<0.001$). The morphology of the attached platelets after 60 min of incubation is displayed as shown in Fig. 4. Si substrate showed a dense platelet layer with predominantly spread platelets (categories IV and V) (Fig. 4(a)), whereas, on F-DLC80, a few platelets adhered, and the categories of platelets uniformly varied between I to V (Fig. 4(c)). DLC films showed that almost all the platelets were categorized into III to V (Fig. 4(b)).

In this present study, DLC and F-DLC coatings could suppress the adhesion and activation of platelets compared to Si substrate. The surface that promoted the greatest spreading of platelets, i.e., the Si substrate, is the most hydrophilic in the tested samples. In contrast, F-DLC coating, which caused less activation, was most hydrophobic in the tested samples. This suggests that the wettability of a biomaterial surface determines in part its blood compatibility. However, it has been described to be influential that blood compatibility is not solely determined by wettability and also the specific chemical composition, interfacial free energy and a higher ratio of albumin/fibrinogen adsorption of biomaterial surfaces [16,17]. The mechanism of biomaterial-associated thrombosis is not fully clear. It is very complicated to determine all factors that contributed to novel antithrombogenic properties of F-DLC films in this study. Further in vitro and in vivo studies are needed to investigate all of the factors related with biomaterial-associated thrombosis.

4. Conclusion

We have presented an engineering analysis of fluorine-doped DLC films and quantitative and morphological studies on platelet adhesion to DLC films or F-DLC coated Si and bare Si substrate incubated in PRP. In this study, we described a novel antithrombogenic effect by doping with fluorine into DLC films compared to Si substrate and conventional DLC. Our experiments showed that an addition of fluorine into DLC films enhanced the water-shedding properties. The number of platelets per unit area decreased in order of Si, DLC and F-DLC80. It was found that F-DLC showed the best antithrombogenicity among the tested samples. In addition, DLC and F-DLC coating inhibited the platelets activation, as well as the number of platelets on the film surface.

The presented F-DLC appears to be a promising candidate coating material for blood contacting devices, such as interventional devices, artificial organs and pace-makers. However, more basic study and long-term implantation are needed.

References

[1] D.L. Fischman, M.B. Leon, D.S. Baim, R.A. Schatz, M.P. Savage, I. Penn, K. Detre, L. Veltri, D. Ricci, M. Nobuyoshi, M. Cleman, R. Heuser, D. Almond, P.S. Teirstein, R.D. Fish, A. Colombo, J. Brinker, J. Moses, A. Shaknovich, J. Hirshfeld, S. Bailey, S. Ellis, R. Rake, S. Goldberg, N. Engl. J. Med. 331 (1994) 496.
[2] P.W. Serruys, P. de Jaegere, F. Kiemeneij, C. Macaya, W. Rutsch, G. Heyndrickx, H. Emanuelsson, J. Marco, V. Legrand, P. Materne, J. Belardi, U. Sigwart, A. Colombo, J.J. Goy, P. van den Heuvel, J. Delcan, M. Morel, N. Engl. J. Med. 331 (1994) 489.
[3] P. Rubartelli, L. Niccoli, E. Verna, C. Giachero, M. Zimarino, A. Fontanelli, C. Vassanelli, L. Campolo, E. Martuscelli, G. Tommasini, J. Am. Coll. Cardiol. 32 (1998) 90.
[4] R. Komatsu, M. Ueda, T. Naruko, A. Kojima, A.E. Becker, Circulation 98 (1998) 224.
[5] L.A. Thomson, F.C. Law, N. Rushton, J. Franks, Biomaterials 12 (1991) 37.
[6] I. Dion, X. Roques, C. Baquey, E. Baudet, B. Basse Cathalinat, N. More, Bio-Med. Mater. Eng. 3 (1993) 51.
[7] H.S. Tran, M.M. Puc, C.W. Hewitt, D.B. Soll, S.W. Marra, V.A. Simonetti, J.H. Cilley, A.J. DelRossi, J. Invest. Surg. 12 (1999) 133.
[8] M.I. Jones, I.R. McColl, D.M. Grant, K.G. Parker, T.L. Parker, Diamond Relat. Mater. 8 (1999) 457.
[9] M.I. Jones, I.R. McColl, D.M. Grant, K.G. Parker, T.L. Parker, J. Biomed. Mater. Res. 52 (2000) 413.
[10] T.I. Okpalugo, A.A. Ogwu, P.D. Maguire, J.A. McLaughlin, Biomaterials 25 (2004) 239.
[11] P. Yang, N. Huang, Y.X. Leng, J.Y. Chen, R.K. Fu, S.C. Kwok, Y. Leng, P.K. Chu, Biomaterials 24 (2003) 2821.
[12] N. Nurdin, P. Francois, Y. Mugnier, J. Krumeich, M. Moret, B.O. Aronsson, P. Descouts, Eur. Cell. Mater. 5 (2003) 17.
[13] R.D. Frank, H. Dresbach, H. Thelen, H.G. Sieberth, J. Biomed. Mater. Res. 52 (2000) 374.
[14] S.L. Goodman, T.G. Grasel, S.L. Cooper, R.M. Albrecht, J. Biomed. Mater. Res. 23 (1989) 105.
[15] R.D. Allen, L.R. Zacharski, S.T. Widirstky, R. Rosenstein, L.M. Zaitlin, D.R. Burgess, J. Cell Biol. 83 (1979) 126.
[16] B.J. Hunt, R. Parratt, M. Cable, D. Finch, M. Yacoub, Blood Coagul. Fibrinolysis 8 (1997) 223.
[17] H.T. Spijker, R. Bos, H.J. Busscher, T.G. von Kooten, W. von Oeveren, Biomaterials 23 (2002) 757.

GENES, CHROMOSOMES & CANCER 42:269–279 (2005)

Identification of a SRC-Like Tyrosine Kinase Gene, *FRK*, Fused with *ETV6* in a Patient with Acute Myelogenous Leukemia Carrying a t(6;12)(q21;p13) Translocation

Noriko Hosoya,[1] Ying Qiao,[1] Akira Hangaishi,[1] Lili Wang,[1] Yasuhito Nannya,[1] Masashi Sanada,[1] Mineo Kurokawa,[1] Shigeru Chiba,[1,2] Hisamaru Hirai,[1,2] and Seishi Ogawa[1,3]*

[1]Department of Hematology and Oncology, Graduate School of Medicine, University of Tokyo, Tokyo, Japan
[2]Department of Cell Therapy and Transplantation Medicine, University of Tokyo Hospital, University of Tokyo, Tokyo, Japan
[3]Department of Regeneration Medicine for Hematopoiesis, Graduate School of Medicine, University of Tokyo, Tokyo, Japan

The SRC family of kinases is rarely mutated in primary human tumors. We report the identification of a SRC-like tyrosine kinase gene, *FRK* (Fyn-related kinase), fused with *ETV6* in a patient with acute myelogenous leukemia carrying t(6;12)(q21;p13). Both reciprocal fusion transcripts, *ETV6/FRK* and *FRK/ETV6*, were expressed. In *ETV6/FRK*, exon 4 of *ETV6* was fused in-frame to exon 3 of *FRK*, producing a chimeric protein consisting of the entire oligomerization domain of ETV6 and the kinase domain of FRK. The ETV6/FRK protein was shown to be constitutively autophosphorylated on its tyrosine residues. ETV6/FRK phosphorylated histones H2B and H4 in vitro to a greater extent than did FRK, suggesting it had elevated kinase activity. ETV6/FRK could transform both Ba/F3 cells and NIH3T3 cells, which depended on its kinase activity. Moreover, ETV6/FRK inhibited ETV6-mediated transcriptional repression in a dominant-negative manner. This report provides the first evidence that a SRC-like kinase gene, *FRK* fused with *ETV6*, could directly contribute to leukemogenesis by producing an oncoprotein, ETV6/FRK, with dual functions: constitutive activation of the ETV6/FRK tyrosine kinase and dominant-negative modulation of ETV6-mediated transcriptional repression.

INTRODUCTION

The *SRC* gene was the first protooncogene isolated as the cellular homologue of v-*SRC*, the retroviral transforming oncogene of avian Rous sarcoma virus (Brown and Cooper, 1996). Since then, it has become clear that *SRC* is the prototype for a family of genes that encode nonreceptor tyrosine kinases implicated in a variety of cellular processes, including cell growth, differentiation, and carcinogenesis. The SRC family of kinases shares common structures consisting of an N-terminal unique domain, SRC homology 3 (SH3) and SRC homology 2 (SH2) domains, a kinase domain, and a short C-terminal regulatory tail (Brown and Cooper, 1996). They are normally maintained in an inactive state through phosphorylation of a critical C-terminal tyrosine residue (Tyr 530 in human SRC, Tyr 527 in chicken SRC) by the C-terminal SRC kinase (Csk) (Brown and Cooper, 1996). The SH3 and SH2 domains also participate in this negative regulation through intramolecular interactions (Brown and Cooper, 1996; Schindler et al., 1999; Xu et al., 1999; Young et al., 2001).

The SRC and its family member kinases have long been postulated to participate in oncogenic processes. Activated variants of SRC family kinases, including the viral oncoprotein v-SRC, are capable of inducing malignant transformation in a variety of cell types (Parker et al., 1984; Cartwright et al., 1987). Activation of SRC-like kinases recently was described in *BCR-ABL1*-expressing acute lymphoblastic leukemia in mice (Hu et al., 2004). Elevated expression and/or activity of SRC have been documented in several types of primary human tumors (Bolen et al., 1987; Ottenhoff-Kalff et al., 1992; Talamonti et al., 1993). However, for many years, structural abnormalities of the SRC family of kinases have been detected rarely in primary human tumors. Although Irby et al. (1999)

Supported by: Research on Human Genome and Tissue Engineering, Health and Labour Sciences Research Grants, Ministry of Health, Labour and Welfare of Japan; Japan Society for the Promotion of Science; Grant number: KAKENHI 14570962.

*Correspondence to: Seishi Ogawa, Department of Hematology and Oncology, Department of Regeneration Medicine for Hematopoiesis, Graduate School of Medicine, University of Tokyo, 7-3-1, Hongo, Bunkyo-ku, Tokyo 113-8655, Japan.
E-mail: sogawa-tky@umin.ac.jp

Received 22 July 2004; Accepted 15 October 2004
DOI 10.1002/gcc.20147
Published online 20 December 2004 in Wiley InterScience (www.interscience.wiley.com).

reported that 12% of advanced human colon cancers had a truncating mutation at codon 531 of the *SRC* gene, determining the importance of this mutation in the generation of colorectal cancers remained elusive according to the negative results in subsequent reports (Daigo et al., 1999; Wang et al., 2000; Laghi et al., 2001). In primary hematopoietic malignancies, no studies have demonstrated structural abnormalities of the SRC family of kinases.

In this study, we performed molecular analysis of a t(6;12)(q21;p13) observed as the sole chromosomal abnormality in a case of acute myelogenous leukemia (AML) and identified a SRC-like tyrosine kinase gene, *FRK* (Fyn-related kinase or *Rak*), on 6q21 (Cance et al., 1994; Lee et al., 1994) that is fused with *ETV6* (also called *TEL*), a gene frequently involved in chromosomal translocations in a variety of human leukemias (Golub et al., 1997). We found that the resultant chimeric protein, ETV6/FRK, is a transforming oncoprotein with elevated kinase activity. We also demonstrated that ETV6/FRK inhibits ETV6-mediated transcriptional repression in a dominant-negative manner, indicating that ETV6/FRK is a unique oncoprotein with dual functions. This is the first report showing the involvement of a SRC-like kinase gene (*FRK*) in primary human cancers.

MATERIALS AND METHODS

Case History

The patient was a 69-year-old Japanese woman with AML-M4, carrying the translocation t(6;12)(q21;p13) as the sole chromosomal abnormality in 8 of 20 examined bone marrow metaphase cells. After obtaining informed consent, a sample of her bone marrow was taken for use in this study. The patient did not respond to chemotherapy and died 5 months later.

Fluorescence In Situ Hybridization Analysis

Fluorescence in situ hybridization (FISH) analysis was performed as previously described (Pinkel et al., 1986) with a panel of biotin- and digoxigenin-labeled cosmid probes that contained different exons of *ETV6*, kindly provided by Dr. Peter Marynen (University of Leuven, Leuven, Belgium). The order and the relative locations of cosmids are depicted in Figure 1A.

3′-Rapid Amplification of cDNA End

To do the 3′-rapid amplification of cDNA end (RACE), total RNA was isolated from the leukemic sample as described previously (Ogawa et al., 1996). First-strand cDNA was synthesized from 2.5 μg of total RNA using the primer R2N6 as described previously by Peeters et al. (1997). The first polymerase chain reaction (PCR) was performed with primers T4F1 and R2N6R1 (Peeters et al., 1997). Then, a diluted product of the first PCR, along with primers T4F2 and R2N6R2, was used for the second, nested PCR (Peeters et al., 1997). The nucleotide sequences of the primers used in this study and the conditions for PCR are listed in Table 1. The PCR products were subcloned into the pCR® 2.1-TOPO® vector using a TOPO TA Cloning® kit (Invitrogen, Tokyo, Japan) and subjected to DNA sequencing by use of a 3100 Applied Biosystems automated sequencer (Applied Biosystems, Chiba, Japan).

Reverse Transcriptase–PCR

For the reverse transcriptase-PCR (RT-PCR), 5 μg of the total RNA was transcribed to cDNA with 2 units of Moloney murine leukemia virus reverse-transcriptase (MMLV-RT, Stratagene, La Jolla, CA) using a random hexamer. One-tenth of the synthesized cDNA was directed to PCR analysis. Primers T4F2 and FRK1198R were used to confirm the *ETV6/FRK* transcripts. The primers for detecting the reciprocal *FRK/ETV6* transcripts were FRK451F and TEL723R. For amplification of the wild-type *ETV6* and *FRK* transcripts, primers T4F2 and TEL723R and primers FRK808F and FRK1198R, respectively, were used. All the sequences of the RT-PCR products were verified by direct sequencing.

Plasmid Construction

Full-length *ETV6* cDNA tagged with a FLAG sequence at the 5′ end, a gift from Dr. Kinuko Mitani (Dokkyo University School of Medicine, Tochigi, Japan), was subcloned into the expression plasmid pME18S-neo (Invitrogen, San Diego, CA). A FLAG-tagged full-length *FRK* cDNA was isolated by RT-PCR from total RNA obtained from human placenta using primers *Eco*RI-FLAG-FRK and FRK-*Not*I-2058R and was cloned into pME18S-neo. The pME18S-neo-FLAG-ETV6/FRK vector was generated by replacement of the *Cla*I-*Not*I fragment of the pME18S-neo-FLAG-ETV6 vector with the *Cla*I-*Not*I fragment of *ETV6/FRK*, which was obtained by RT-PCR from the patient's bone marrow using primers TEL-*Cla*I-F and FRK-*Not*I-2058R, with subsequent digestion with *Cla*I and *Not*I. To construct a kinase-inactive mutant of ETV6/FRK, designated ETV6/FRK(K262R), a point mutation corresponding

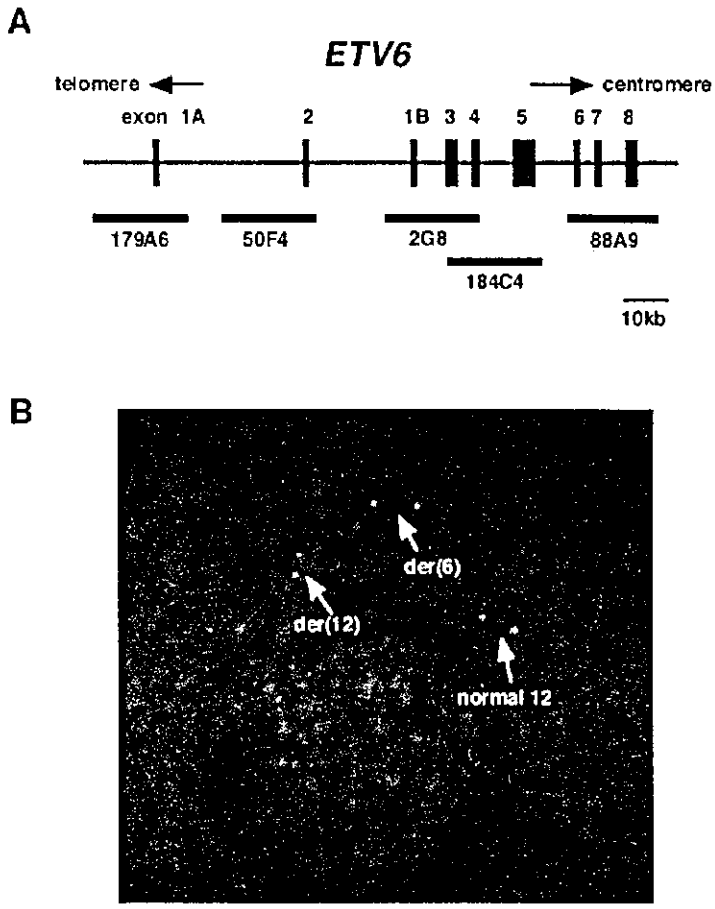

Figure 1. Analysis of breakpoint on chromosome 12. (A) A genomic map of *ETV6* and location of the cosmid probes used for FISH analysis. (B) FISH analysis of the patient's leukemic cells. The signals of the 2G8 probe (red) containing *ETV6* exons 1B, 3, and 4 are hybridized on the der(6) and on the normal 12p, whereas those of the 184C4 probe (green) containing *ETV6* exons 3–5 are found on the der(6), the der(12), and the normal 12p.

to a kinase-inactivating mutation in the ATP-binding site lysine residue (Lys262) of FRK was introduced into *ETV6/FRK* cDNA. A mutated fragment generated by PCR using the mutagenic primer FRK-K262R-*Bam*HI and the primer TEL-*Eco*RI-FLAG was spliced together with a C-terminal partial fragment of *FRK* into pME18S-neo. A FLAG-tagged full-length *FRK/ETV6* cDNA was constructed into the pME18S-neo vector by assembling partial fragments from *ETV6* and *FRK* and a fragment spanning the *FRK/ETV6* junction generated by RT-PCR using primers FRK451F and TEL723R. All the constructs were sequenced to confirm the fidelity of the sequence and conservation of the reading frame at the site of fusion.

Cell Lines, Transfection, and Cell Transformation Studies

For transient expression studies, 4×10^4 HeLa cells were seeded in each 60-mm dish and transfected with expression plasmid or plasmids 24 hr later by a lipofection method using Effectine™ Transfection Reagent (Qiagen, Hilden, Germany). Cells were incubated for 48 hr and harvested for analysis. NIH3T3 cells were transfected with expression plasmids, also using Effectine™, and selected in 400 μg/ml of G418 for 2 weeks. Ba/F3 clones stably expressing ETV6/FRK or other proteins were obtained by electroporation of each expression plasmid into Ba/F3 cells as previously described (Carroll et al., 1996) and subsequent isolation of individual G418-resistant subclones by limiting dilution. Expression of the transfected genes was evaluated by immunoblotting as previously described (Maki et al., 1999) using anti-FLAG-M2 monoclonal antibody (Sigma-Aldrich, St. Louis, MO). The soft-agar colony assay was performed as previously described (Kurokawa et al., 1996). After 21 days, all macroscopic colonies larger than 0.25 mm in diameter were counted. For growth curves, 2×10^4 G418-resistant Ba/F3 cells were washed 3 times with PBS and plated in IL-3-free medium on day 0, and viable cells were counted each day by trypan blue exclusion.

TABLE I. Primers Used For 3′-RACE and (RT)-PCR Amplifications

Name	Sequence
R2N6	5′-CCAGTGAGCAGAGTGACGAGGACTCGAGCTCAAGC(N)6-3′
T4F1	5′-CATATTCTGAAGCAGAGGAAA-3′
R2N6R1	5′-CCAGTGAGCAGAGTGACG-3′
T4F2	5′-ACACAGCCGGAGGTCATACT-3′
R2N6R2	5′-GAGGACTCGAGCTCAAGC-3′
FRK1198R	5′-CTTCCCATACTTCGCAAAC-3′
FRK451F	5′-AGCAACATCTGTCAGAGGCT-3′
TEL723R	5′-GTAGGACTCCTGGTGGTTGTT-3′
FRK808F	5′-ATCGGAAGATCAGATGCAGAG-3′
*Eco*RI-FLAG-FRK	5′-GCGAATTCGTTGTGATGGGGGACTACAAGGACGAC GATGACAAGTCCGGGAGCAACATCTGTCAGAGGCT-3′
FRK-*Not*I-2058R	5′-ATTGCGGCCGCACTGATTGTGCAGTTGGTTGA-3′
TEL-*Cla*I-F	5′-CTTTCGCTATCGATCTCCTCA-3′
TEL-*Eco*RI-FLAG	5′-GCGAATTCGTTGTGATGGGGGACTACAAGGACGAC GATGACAAGTCCGGGTCTGAGACTCCTGCTCAGTG-3′
FRK-K262R-*Bam*HI	5′-TTGGATCCATTGAACCTGGTTTTAATGTTCTCACTG-3′

Thermal cycling profile was: 94°C for 2 min, followed by 35 cycles of 94°C for 1 min, 60°C for 1 min and 72°C for 2 min, with a final extension at 72°C for 10 min.

Immunoprecipitation, Immunoblotting, and Immune Complex Kinase Assay

Lysates were prepared by washing cells (1×10^6–1×10^7) with phosphate-buffered saline and then adding lysis buffer [10 mM Tris-HCl (pH 7.4), 150 mM NaCl, 1.0% NP-40, 1 mM EDTA, and 1 mM Na3VO4] containing 5 mM phenylmethyl-sulfonylfluoride and 1 μg/ml of aprotinin. After 10 min on ice, the samples were centrifuged at 12,000 g to remove insoluble particles. For immunoprecipitation, 1 mg of total cell lysate was incubated with anti-FLAG-M2 antibody for 1 hr at 4°C, after which 50 μl of Protein G-Sepharose beads (Amersham Biosciences, Uppsala, Sweden) was added. After rotating for 1 hr at 4°C, immunoprecipitates were washed 3 times and boiled in loading buffer for 5 min. Protein samples were separated on 6.5%–15% gradient SDS-polyacrylamide gels and transferred onto PVDF membranes (Millipore, Bedford, MA). Immunoblotting was performed as previously described (Maki et al., 1999) using either anti-FLAG-M2 antibody or antiphosphotyrosine monoclonal antibody 4G10 (Upstate Biotechnology Incorporated, Lake Placid, NY) as a primary antibody.

For the immune complex kinase assay, immunoprecipitates were washed 3 times and suspended in kinase buffer [40 mM HEPES (pH 7.4), 10 mM $MgCl_2$, 5 mM $MnCl_2$]. For determination of kinase activity, 2.5 μg of either histone H2B or histone H4 (Roche Diagnostics K. K., Tokyo, Japan) was added to each reaction. Kinase reactions were initiated by the addition of 10 μCi of [γ-^{32}P] ATP (3,000 Ci/mmol; Amersham Biosciences Corp., Piscataway, NJ) and incubated at 30°C for 15 min. Reactions were stopped by the addition of loading buffer and analyzed by SDS-PAGE and exposure to a film.

Luciferase Assay

For the luciferase assay, 4×10^4 HeLa cells were transfected with 1 μg of the reporter plasmid (EBS)3tkLuc (Waga et al., 2003), a kind gift of Dr. Kinuko Mitani, along with the indicated amounts of the expression vectors. The total amount of DNA in weight was adjusted to be equal by adding pME18S-neo plasmid. Luciferase activities were determined as described previously (Maki et al., 1999). All transfection experiments were performed in duplicate at least 3 times.

RESULTS

Identification of the Breakpoint on Chromosome 12

We performed FISH experiments using several probes from the *ETV6* locus, on 12p13 (Fig. 1A). The signals from the cosmids containing exons 1–4 (179A6, 50F4, and 2G8) were found on the der(6) (Fig. 1B), whereas the signals from the cosmid containing exons 3–5 (184C4) were split to the der(6) and the der(12) (Fig. 1B), suggesting that the breakpoint on 12p13 was localized to *ETV6* exons 4–5. The signals on the normal 12p were always observed with all the indicated cosmid probes of the *ETV6* locus, suggesting that the non-

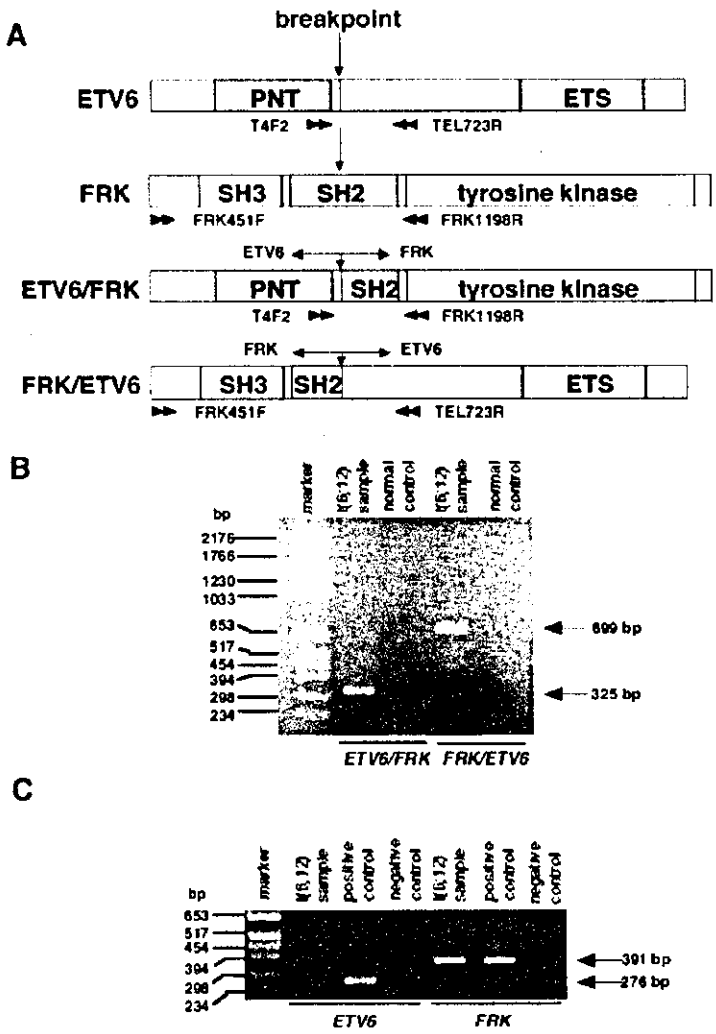

Figure 2. Identification of *ETV6/FRK* and *FRK/ETV6* fusion transcripts. (A) Schematic representation of wild-type *ETV6*, *FRK*, and the fusion transcripts. The breakpoints are indicated by vertical arrows. Horizontal arrows indicate the positions of RT-PCR primers (described in the Materials and Methods section). (B) Detection of *ETV6/FRK* as well as *FRK/ETV6* fusion transcripts by RT-PCR in the patient's leukemic sample. (C) Expression of *ETV6* and *FRK* in the patient's leukemic sample by RT-PCR.

translocated allele of *ETV6* was grossly intact with no large deletions.

Identification of the Fusion Partner of *ETV6*

To identify the unknown fusion partner of *ETV6*, 3′-RACE-PCR was performed. After two rounds of PCR, 3′-RACE-PCR products were successfully obtained. Sequencing analysis of the PCR products showed that exon 4 of *ETV6* was fused to exon 3 of *FRK* on 6q21, creating an *ETV6/FRK* fusion gene. The *FRK* gene encodes a SRC-like nonreceptor tyrosine kinase, consisting of the N-terminal SH3 and SH2 domains, the C-terminal kinase domain, and a short regulatory tail (Fig. 2A). The *ETV6/FRK* fusion gene produced a chimeric protein in which the entire pointed (PNT) oligomerization domain (also called helix–loop–helix domain) of ETV6 and the kinase domain of FRK were fused in-frame (Fig. 2A).

Detection of the *ETV6/FRK* and *FRK/ETV6* Fusion Transcripts

RT-PCR analysis was performed to confirm the fusion transcripts of the *ETV6* and *FRK* genes. Both reciprocal fusion transcripts, *ETV6/FRK* and *FRK/ETV6*, were specifically amplified from the leukemic sample but not from control bone marrow (Fig. 2B). Expression of wild-type *ETV6* and *FRK* also was detected in the leukemic sample (Fig. 2C). There were no mutations in the entire coding sequences of *ETV6*, *FRK*, *ETV6/FRK*, and *FRK/ETV6* (data not shown).

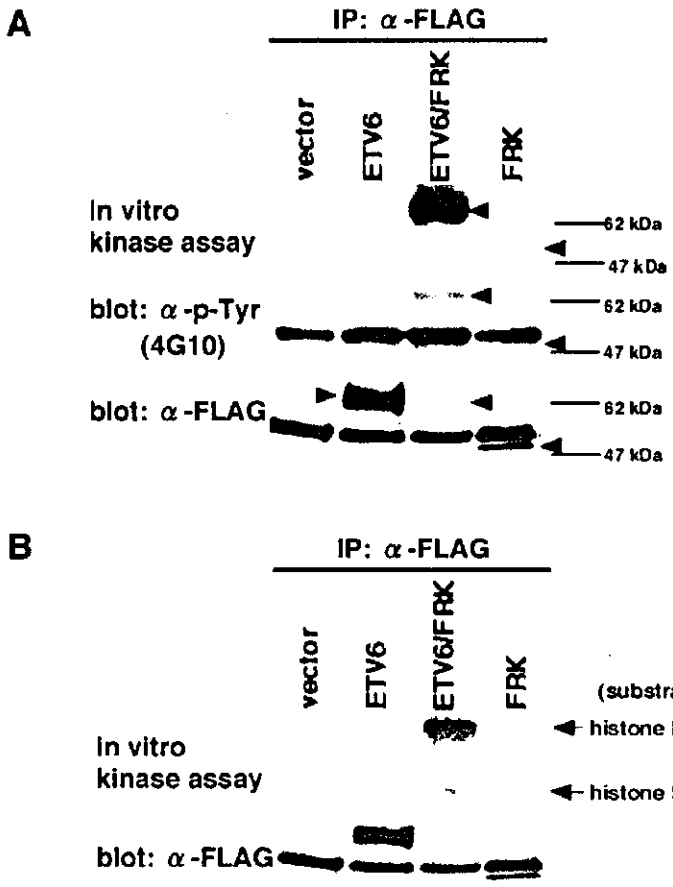

Figure 3. The ETV6/FRK tyrosine kinase is constitutively activated in HeLa cells. (A) Lysates of HeLa cells transfected with the indicated expression vectors were immunoprecipitated with an anti-FLAG-M2 monoclonal antibody and then analyzed by immune complex kinase assay (top) or immunoblotting with an antiphosphotyrosine antibody 4G10 (middle). The total amount of each protein was also assessed by immunoblotting with anti-FLAG-M2 antibody (bottom). Arrowheads show the proteins expressed or phosphorylated at an expected size. (B) Results of kinase assay performed with histones H2B (top) and H4 (middle).

Constitutive Activation of the ETV6/FRK Tyrosine Kinase

Because the ETV6/FRK fusion protein retained the kinase domain but lacked the SH3 domain and most of the SH2 domain, we examined its kinase activity. First, we compared the autophosphorylation status of ETV6/FRK and wild-type FRK. Either the ETV6/FRK fusion protein, wild-type FRK, or wild-type ETV6 FLAG-tagged at the N-terminus was introduced into HeLa cells, immunoprecipitated with an anti-FLAG-M2 monoclonal antibody, and then analyzed by the kinase assay or immunoblotting with an antiphosphotyrosine antibody 4G10 (Fig. 3A, top and middle). To compare expression levels, the same amounts of immunoprecipitate were also subjected to anti-FLAG blot (Fig. 3A, bottom). A high level of tyrosine phosphorylation occurred only in the ETV6/FRK protein (Fig. 3A, top and middle). A basal level of autophosphorylation also was detectable in the wild-type FRK (Fig. 3A, top), a finding in agreement with the previous data (Cance et al., 1994). However, the level of autophosphorylation was significantly lower than that of ETV6/FRK (Fig. 3A, top and middle). Next, we compared the ability of ETV6/FRK and wild-type FRK to phosphorylate exogenous substrates. When histone H2B or H4 was added to the kinase reaction, they were found to be phosphorylated to a greater extent in ETV6/FRK-expressing cells than in FRK-expressing cells (Fig. 3B), suggesting that the ETV6/FRK protein had elevated tyrosine kinase activity.

Cell Transformation by ETV6/FRK in a Kinase-Dependent Manner

To assay the transforming activities of ETV6/FRK, we stably expressed the cDNA-encoding ETV6/FRK or other proteins into the fibroblast cell line NIH3T3. We established 3 NIH3T3 clones expressing ETV6/FRK, 2 clones expressing FRK/ETV6, 2 clones expressing FRK, 2 clones expressing ETV6, and 2 clones expressing ETV6/FRK(K262R) (Fig. 4A), the kinase-inactive

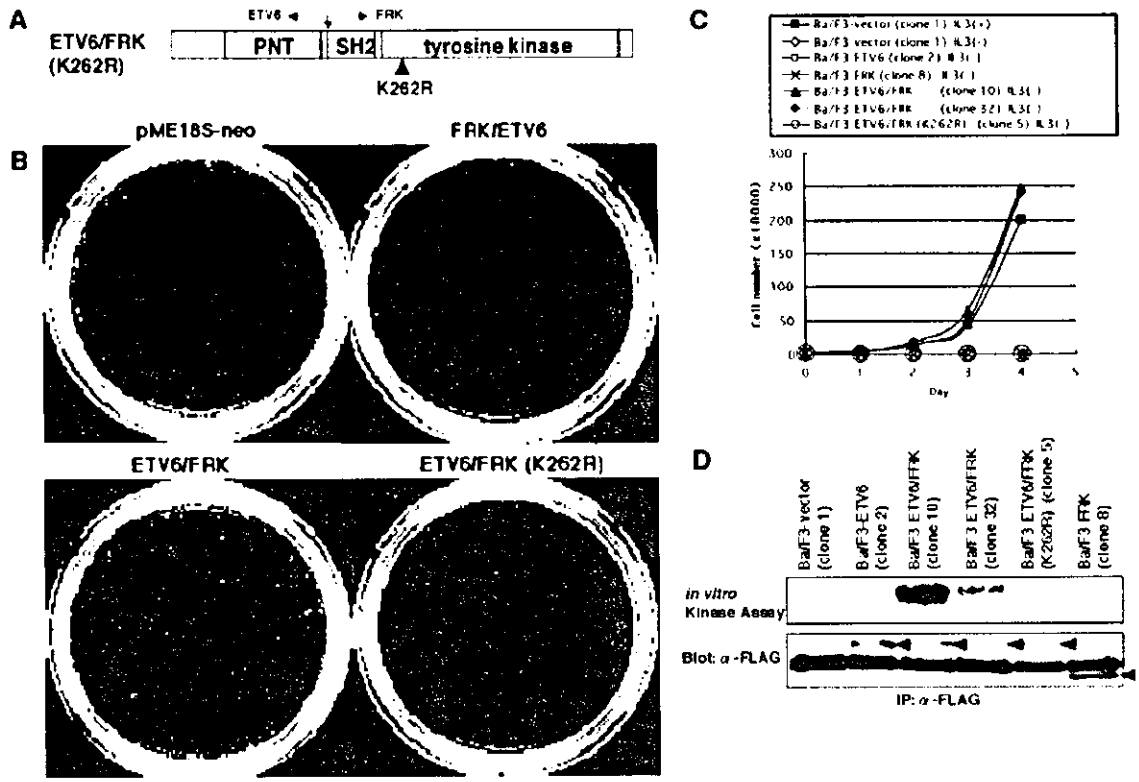

Figure 4. ETV6/FRK transforms NIH3T3 cells and Ba/F3 cells in a kinase-dependent manner. (A) Schematic representation of the kinase-inactive ETV6/FRK(K562R) mutant with a lysine-to-arginine mutation at the ATP binding site. (B) Soft-agar assay demonstrating macroscopic colony formation in ETV6/FRK-expressing NIH3T3 cells. (C) 2 × 10^4 Ba/F3 cells stably transfected with the indicated expression vectors were washed free of IL-3 and plated on day 0 in growth medium without IL-3. Viable cells were counted each day. Data of the representative clone(s) for each protein are presented. (D) Cell lysates of the indicated Ba/F3 clones were immunoprecipitated with an anti-FLAG-M2 antibody and then subjected to kinase assay (top) and immunoblotting with anti-FLAG-M2 antibody (bottom). Arrowheads show the proteins expressed at an expected size.

mutant of ETV6/FRK, confirmed by immunoblotting analysis (data not shown). The soft-agar assay was performed on each clone. Comparable results were obtained for the clones expressing the same proteins, and the representative data are presented. Only the NIH3T3 cells expressing intact ETV6/FRK were able to produce macroscopic colonies, whereas the NIH3T3 cells transfected with the empty vector or cells expressing the kinase-inactive mutant ETV6/FRK(K262R), the reciprocal FRK/ETV6 fusion protein, wild-type FRK, or wild-type ETV6 failed to grow colonies (Fig. 4B, Table 2). These results suggest that ETV6/FRK but not FRK/ETV6 contributes to neoplastic transformation in a kinase-dependent manner.

Next, we also examined the ability of ETV6/FRK to transform the murine hematopoietic cell line Ba/F3, which is strictly dependent on IL-3 for survival and proliferation. Following stable transduction by electroporation, we obtained 6 Ba/F3 clones expressing ETV6/FRK, 2 clones expressing FRK, 2 clones expressing ETV6, and 3 clones expressing ETV6/FRK(K262R), confirmed by immunoblotting analysis (data not shown). To assay the ability to confer independent proliferation of IL-3, each Ba/F3 clone was switched to growth medium without IL-3. Comparable results were obtained for the clones expressing the same proteins, and the representative data are presented. The Ba/F3 clones expressing ETV6/FRK showed sustained proliferation in the absence of IL-3 (Fig. 4C). In contrast, Ba/F3 cells transfected with the empty vector or cells expressing kinase-inactive mutant ETV6/FRK(K262R), wild-type FRK, and wild-type ETV6 were all unable to proliferate in the absence of IL-3 (Fig. 4C). Although the ETV6/FRK proteins expressed in the stable clones were constitutively autophosphorylated, the ETV6/FRK(K262R) mutants were not (Fig. 4D). These observations indicate that ETV6/FRK is a dominant oncoprotein and that constitutive activa-

TABLE 2. Transformation of NIH3T3 Cells By ETV6/FRK

Transfected DNA	No. of colonies[a]
pME18S-neo (vector)	0
pME18S-neo-ETV6	0
pME18S-neo-FRK	0
pME18S-neo-ETV6/FRK	15
pME18S-neo-ETV6/FRK(K262R)	0
pME18S-neo-FRK/ETV6	0

NIH3T3 cells were transfected with the indicated constructs, and stable transfectants were selected in G418. Cells were plated in soft agar. Macroscopic colonies were counted at day 21.
[a]Average of four experiments.

tion of the ETV6/FRK tyrosine kinase is necessary for ETV6/FRK-induced transformation.

Inhibition of ETV6-Mediated Transcription Repression by ETV6/FRK

Because ETV6 is an ETS transcription factor that acts as a transcriptional repressor (Lopez et al., 1999), we also investigated the transcriptional regulatory property of ETV6/FRK and its ability to modulate the function of wild-type ETV6. We transfected a previously described (EBS)3tkLuc reporter, in which the luciferase gene is placed under the control of an ETS responsive promoter (Waga et al., 2003), along with either wild-type ETV6, ETV6/FRK, or FRK/ETV6 into HeLa cells and evaluated luciferase activity. The results showed, in agreement with the previous finding (Waga et al., 2003), that there was decreased luciferase activity after cotransfection of (EBS)3tkLuc with the wild-type ETV6 expression plasmid (Fig. 5A). In contrast, no repression was observed when ETV6/FRK or FRK/ETV6 was expressed with the (EBS)3tkLuc reporter (Fig. 5A).

Because the oncoprotein ETV6/FRK lacks the ETS DNA binding site but still retains the PNT oligomerization domain, it is possible that it might affect ETV6-mediated transcriptional repression by heterodimerizing with ETV6. Notably, coexpression of ETV6/FRK abolished the transcriptional repression by ETV6 in a dose-dependent manner (Fig. 5B), suggesting that ETV6/FRK has a dominant-negative effect on ETV6-mediated transcriptional repression. In contrast, coexpression of the reciprocal FRK/ETV6 protein did not affect ETV6-mediated transcriptional repression (Fig. 5B). In control experiments, dose-dependent expression of the ETV6, ETV6/FRK, or FRK/ETV6 protein was confirmed by immunoblotting analysis (data not shown).

DISCUSSION

The t(6;12)(q21;p13) is a rare but recurrent reciprocal chromosome translocation in human leukemia (Hayashi et al., 1990; Katz et al., 1991; Raimondi et al., 1997). In this article, we report our finding that it generated novel fusion genes *ETV6/FRK* and *FRK/ETV6* in a case of AML. FRK belongs to a family of SRC kinases, as at the amino acid level, it has the highest homology, 50%, with FYN (Cance et al., 1994; Lee et al., 1994). Although several tyrosine kinase (TK) genes have been identified as fusion partners of *ETV6* (Golub et al., 1994; Papadopoulous et al., 1995; Lacronique et al., 1997; Peeters et al., 1997; Cazzaniga et al., 1999; Eguchi et al., 1999; Iijima et al., 2000; Kuno et al., 2001), this is the first report of a SRC-family tyrosine kinase gene being fused with *ETV6* and structurally altered in human cancers. In the resultant ETV6/FRK fusion protein, the entire PNT oligomerization domain of ETV6 and the kinase domain of FRK are fused in frame. We demonstrated that this ETV6/FRK fusion protein constitutively underwent autophosphorylation on its tyrosine residues. ETV6/FRK had elevated kinase activity compared to that in wild-type FRK. ETV6/FRK showed transforming activities in two cell lines, Ba/F3 and NIH3T3, indicating that ETV6/FRK is a dominant transforming oncoprotein. The kinase-inactive mutant ETV6/FRK(K262R) transformed neither of these two cell lines, indicating that the kinase activity of ETV6/FRK was essential for transformation. The reciprocal fusion protein FRK/ETV6, whose mRNA also was transcribed in the patient sample, did not have transforming activity. These data strongly suggest that the elevated kinase activity of the ETV6/FRK fusion protein directly contributes to the pathogenesis of leukemia with a t(6;12)(q21;p13).

Although activated variants of the SRC family kinases show transforming activities (Parker et al., 1984; Cartwright et al., 1987), the *SRC* and its family of genes rarely have been reported as being mutated or structurally altered in primary human tumors. Irby et al. (1999) reported that 12% of advanced human colon cancers in the United States had a truncating mutation at codon 531 of the *SRC* gene and that the mutation elevated kinase activity and promoted the potential for malignancy. However, three subsequent large-scale studies on advanced colorectal cancers in Japanese, northern European, Chinese, and Italian patients failed to detect the mutation (Daigo et al., 1999; Wang et al., 2000; Laghi et al., 2001), making the

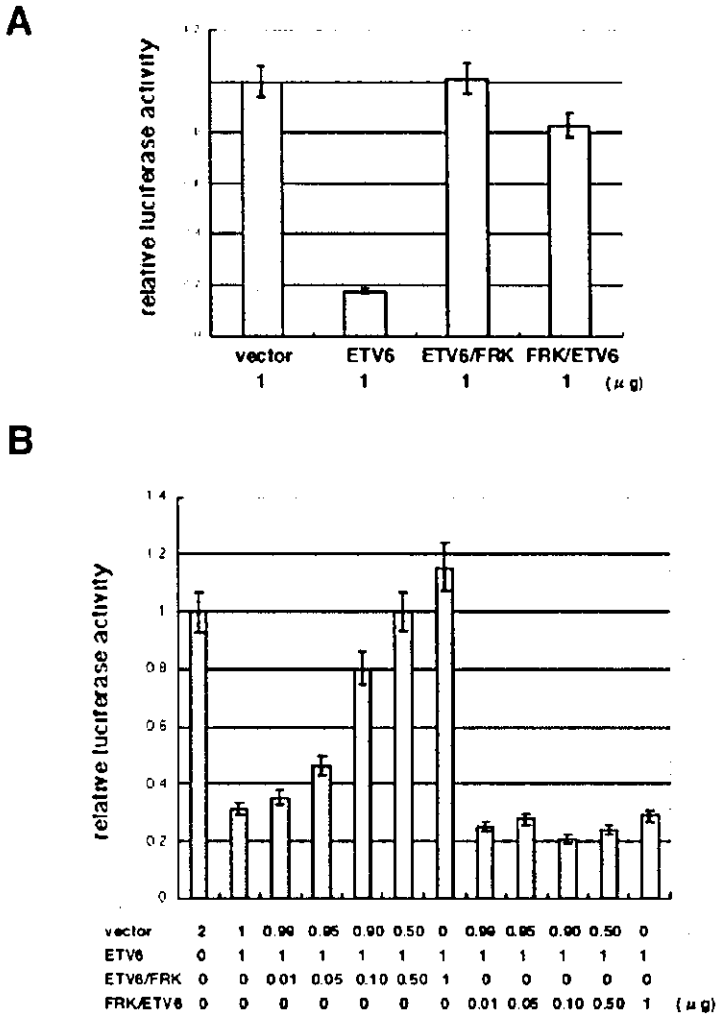

Figure 5. ETV6/FRK is a dominant-negative regulator of ETV6-mediated transcriptional repression in HeLa cells. (A) HeLa cells were transfected with 1 μg of (EBS)3tkLuc reporter plasmid along with 1 μg of the indicated expression vector. Bars show relative luciferase activities to the level when a control plasmid pME18S-neo was cotransfected with the corresponding reporter plasmid, and they present average results of duplicate experiments. (B) HeLa cells were transfected with 1 μg of (EBS)3tkLuc reporter plasmid along with 1 μg of pME-18S-neo-FLAG-ETV6 expression vector together with indicated amounts of pME18S-neo-FLAG-ETV6/FRK or pME18S-neo-FLAG-FRK/ETV6 expression vector. The results are presented as relative luciferase activities.

importance of this mutation controversial. In hematopoietic malignancies, two human T-cell acute lymphoblastic leukemia cell lines have been shown to have rearrangement of *LCK*, a SRC-family kinase gene (Tycko et al., 1991; Wright et al., 1994). In these two cell lines, HSB-2 and SUP-T12, the upstream promoter of the *LCK* gene was juxtaposed to the *TCRB* locus without any accompanying large structural abnormality of the LCK protein. *LCK* mRNA was elevated in the two cell lines (Tycko et al., 1991), and the HSB-2 cell line was later shown to carry several activating point mutations in the *LCK* gene (Wright et al., 1994), indicating that overexpression and/or activation of the LCK kinase would lead to cell transformation. On the other hand, the involvement of SRC family members in primary leukemia has not been reported previously. In this study, we showed that the structural abnormality of an SRC-like kinase gene, *FRK*, through translocation with *ETV6* can directly contribute to leukemogenesis through activation of the altered tyrosine kinase. In addition to the analysis of the current case with a t(6;12), we also performed a mutation analysis of the *FRK* gene in 20 hematopoietic cell lines but failed to detect activating mutations or structural abnormalities (data not shown). Thus, it is currently unclear whether FRK could be activated through other mechanisms such as activating mutations or translocations with other partner gene(s), although more intensive analyses may be required.

Two mechanisms could contribute to the constitutive activation of the ETV6/FRK kinase. First, in the ETV6/FRK fusion protein, the SH3 and SH2 domains of FRK are lost or disrupted, respec-